

EFFECT OF THE RATIO OF CUTTING DEPTH TO EDGE DIAMETER ON CHIP FORMATION MECHANISM IN MACHINING OF CFRPS

Youliang Su, Fuji Wang, Zhenyuan Jia, Junwei Yin, Rao Fu, Bin Niu, and Wei Liu

The Key Laboratory for Precision and Nontraditional Machining Technology of Ministry of Education,
Dalian University of Technology, Dalian, China

Email: suyl@mail.dlut.edu.cn, wfjssl@dlut.edu.cn, jzyxy@dlut.edu.cn, dlyjw@mail.dlut.edu.cn,
fr200761854@mail.dlut.edu.cn, niubin@dlut.edu.cn, lw2007@dlut.edu.cn, web page:
<http://www.dlut.edu.cn/>.

Keywords: CFRPs, chip formation mechanism, cutting depth, edge diameter, subsurface damage

Abstract

Carbon fiber reinforced plastics (CFRPs) are used widely to reduce the structural weight. Drilling and milling processes are inevitable in order to satisfy the assembly requirements of CFRPs structure. However, the subsurface damage easily occurs due to the interface debonding under the cutting forces in machining of CFRPs, and severely reduces the mechanical properties of the structure. This paper studies the chip formation mechanism in machining of CFRPs. Firstly, the characteristic of cutting forces and the specific energy under different ratios of cutting depth to cutting edge diameter (RDD) are investigated by the orthogonal machining of CFRPs. Furthermore, the tool-material interactions are analyzed to investigate the chip formation mechanism. In addition, the fiber failure and the interface debonding are analyzed by the scanning electron microscope (SEM) of the machined surface. For 90° cutting angle, fiber failure mode is like microbuckling due to the insufficient support of the matrix for RDD=1, and the interface debonding does not extend to the subsurface. It changes into the kinkband formation with the increasing of the RDD. For 135° cutting angle, mode I fracture of the interface easily occurs due to the opening load with the increasing of the RDD. Thus, the RDD should be controlled to reduce the severe subsurface damage in machining of CFRPs.

1. Introduction

Carbon fiber reinforced plastics (CFRPs) have the advantages of having a higher specific strength compared to metals and reducing the structural weight of aircraft [1]. CFRPs are usually fabricated to near net shapes by autoclave, compression molding or filament winding. However, a large number of drilling and milling processes are inevitable in order to satisfy the dimensional tolerance and the assembly requirements [2]. Due to the anisotropic characteristic of CFRPs, the subsurface damage caused by the fiber-matrix debonding comes into being so easily in machining of CFRPs [3]. It severely reduces the mechanical properties of CFRPs [4,5]. CFRPs are increasingly applied in the main structure of aircraft, such as the wing covers and fuselage section. With the increasing of the size of the structure, the damage criterion today is so small as to be almost nonexistent due to the tremendous loads. Thus, the nature of the damage in the chip formation must be studied, and the damage will be reduced by choosing the suitable machining parameters.

Chip formation in machining of CFRPs is widely studied in the literature. Fiber orientation is a major factor affecting the chip formation. Two basic failure mechanism at macro level are suggested: shearing in the perpendicular direction of fiber and buckling in the parallel direction of fiber [6]. The main mechanisms preceding the chip separation versus the fiber orientation are summarized in the following modes: delamination type chip formation occurs for 0 fiber orientation, fiber cutting type chip formation occurs for 0° to 90° fiber orientation, the chip formation is dominated by macro fracture

Youliang Su, Fuji Wang, Zhenyuan Jia

for 105° to 150° fiber orientation [7]. It is found that the subsurface damage comes into being so easy for 90° and 135° fiber orientations due to the large cutting forces [8, 9]. Furthermore, the effect of machining parameters and tool geometry on the damage are also investigated. Nakayama at al. study the effects of the cutting edge radius and relief angle on the depth of deformed part for 0 to 90 fiber orientations [10]. The results reveal that a tool with a large cutting edge radius obtain deeper depth of deformed part, but the relief angle could not provide significant effects on depth of deformed part. Zhang at al. reveals that the subsurface damage is related to the depth of cut and rake angle, and at a larger depth of cut (e.g. 50µm and 100µm), the sub-surface damage becomes more severe when the fiber orientation is between 120 and 150 [11]. Furthermore, Jahromi at al. the subsurface damage decreases with the increasing of the angle from 5 to 20 [12]. Furthermore, Q. An finds that the cutting and thrust forces increase with the increase of the cutting edge radius, especially when the cutting edge radius is larger than the depth of cut [13].

Consequently, the cutting edge radius and the depth of cut affects the subsurface damage significantly. In addition, the strength of fiber becomes higher to satisfy the load performance of the main structure [14], such as T800H and IM7. The gap of strength between the fiber and the interface becomes larger accordingly. The interface debonding between the fiber and matrix is more likely to happen due to the large cutting forces in the chip formation for machining of high strength CFRPs. Thus, this paper presents an experimental investigation on the effect of the ratios of cutting depth and cutting edge diameter (RDD) by the orthogonal cutting of the high-strength CFRPs. The cutting forces and the micro topography of the machined surface are measured. Furthermore, based on the compare of the characteristic of cutting forces and the specific energy under different RDDs, tool-material interactions are analyzed to investigate the chip formation mechanism. Finally, the failure of the fiber and matrix are discussed by the micro topography analysis.

2. Experiment setup

The orthogonal cutting experiments are conducted to investigate the chip formation in machining of CFRPs. The angle formed by rotating from the cutting direction to fiber orientation is defined as the cutting angle (θ) as shown in Figure 1. Meanwhile, the angle formed by rotating from the resultant force to the fiber orientation is defined as the angle of action (λ_e). As mentioned above, the subsurface damage for 90° to 135° is serious in machining of CFRPs. This study obtains the orthogonal machining of unidirectional CFRP for 90° and 135° cutting angles. The work piece is fixed on the table of the linear motor, and moves in linear motion providing a steady cutting motion as shown in Figure 1. The cutting tool is fixed on the dynamometer table. The cutting forces are measured by a six-dimensional dynamometer Kistler 9327C. The measured force are divided into two components as follows the cutting force (F_c) and the thrust force (F_t).

Generally, the cutting tool with a lager rake angle can reduce the machining damage[12]. Meanwhile, there is no effect of the relief angle on the machining quality[10]. However, the choice of the relief angle should take account of the tool wear caused by the bouncing back of the fiber. Furthermore, the diameter of the cutting edge should be close to the one of fiber[14]. As a result, the tool geometries used in this paper are shown in Table 1, and the tool material is cemented carbide. The unidirectional CFRP work material used in this study is fabricated from the TORAYCA prepregs with T800 carbon fiber. The UD-CFRPs laminates with 24 polies have a thickness of 3mm and are cut into 40×100mm sheets. Two types of UD-CFRPs laminate of 0° and 45° fiber orientation are selected as shown in Figure 2. Consequently, the experimental conditions are conducted to investigate the effect of RDD on the chip formation as shown in Table 1.

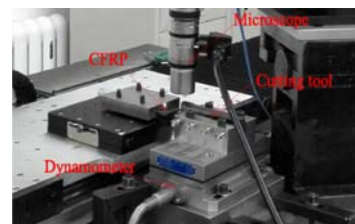
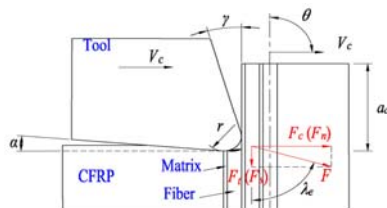


Figure 1. Diagram of orthogonal cutting of UD-CFRP. **Figure 2.** Experimental setup.

Table 1. Machining parameters and tool geometry.

Parameters	Value
Cutting angle ($\theta / ^\circ$)	90, 135
Depth of cut ($a_c / \mu\text{m}$)	10, 30, 50
Diameter of cutting edge ($d_e / \mu\text{m}$)	10
Rake angle ($ / ^\circ$)	25
Relief angle ($ / ^\circ$)	5

3. Results and Discussions

The measured cutting forces are very different under different RDDs as shown in Figure 3. The process of chip formation is smooth just as the ductile material for RDD=1. With the increasing of RDD the degree of the cutting forces fluctuation increases. It reveals that the chip formation mechanism changes accordingly, and the machining responses should be investigated to understand it.

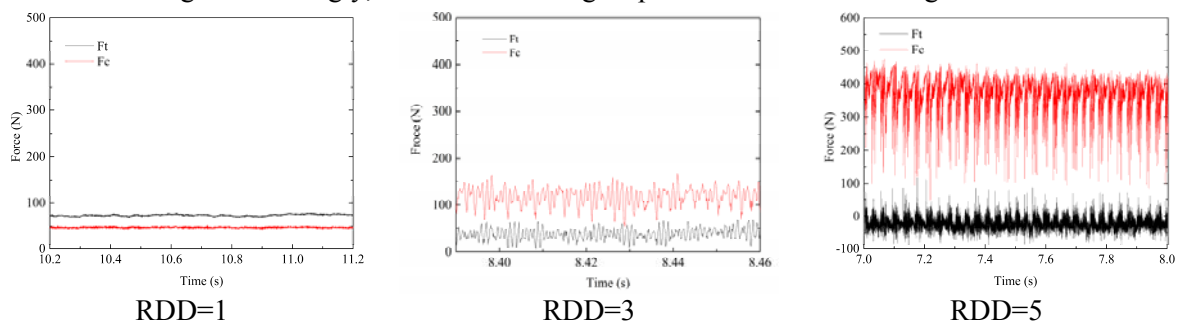


Figure 3. Time series signals of the cutting forces for $\theta = 90^\circ$.

3.1. Characteristics of Cutting Forces

For 90° cutting angle, the thrust force is larger than the cutting force when RDD=1. With the increase of RDD, the cutting force increases all the time. However, the thrust force increases firstly and then decreases. Meanwhile, its direction is reversed when the RDD=5, and its value is far less than the one of the cutting force as shown in Figure 4. For 135° cutting angle, the thrust force is smaller than that for 90° cutting angle, but the cutting force is larger than that for 90° cutting angle when RDD=1. It is different from the phenomenon for 90° cutting angle that the cutting force is far greater than the thrust force. With the increase of RDD, the increase of the cutting force (Fc) is faster than the one for 90° cutting angle obviously. The thrust force direction is reversed in case of RDD=3.

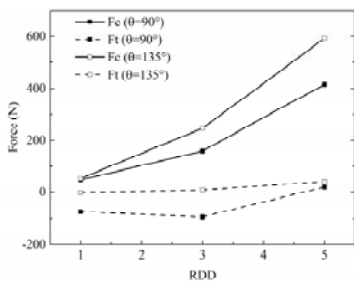


Figure 4. Cutting forces under different RDDs.

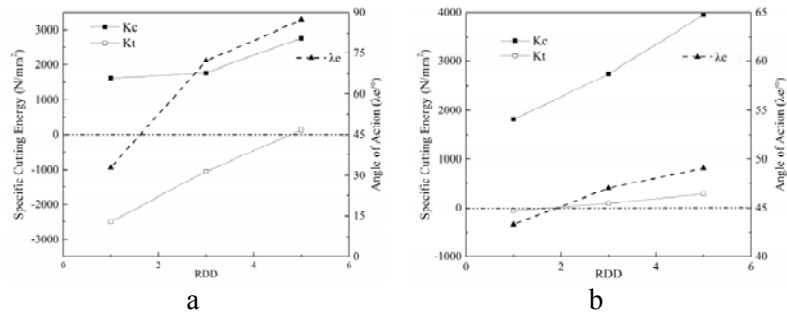


Figure 5. Specific cutting energy and angle of different RDDs: a) $\theta = 90^\circ$, b) $\theta = 135^\circ$.

Furthermore, the Specific Energy (K) required for different mechanisms of chip formation are also discussed. It is the energy required for the removal of unit volume. It can reveal the failure mechanism in the process of chip formation. Figure 5 shows the Specific Energy required for chip formation of

different RDDs for 90° and 135° cutting angles. For 90° cutting angle, the specific cutting energy (K_c) increases with the increasing of RDD on the whole. Contrarily, the specific thrust energy (K_t) decreases with the increasing of RDD. The specific cutting energy (K_c) for RDD=1 is nearly equal to that for RDD=3, and then a substantial rise occurs for RDD=5. It reveals the chip formation mechanism changes with the increasing of RDD from 1 to 5. However, the specific cutting energy (K_c) presents a linear growth for 135° cutting angle, but the specific thrust energy (K_t) barely changes with the increasing of RDD. The specific cutting energy (K_c) for 135° is larger than that for 90° cutting angle obviously once $RDD \geq 3$. It reveals that the bending-dominant chip formation needs more energy than the cutting-dominant one. In addition, the energy is used to press the work material when $RDD < 5$ for 90 cutting angle and $RDD < 3$ for 135 cutting angle. However, the energy is used to raise the work material when $RDD = 5$ for 90 cutting angle and $RDD \geq 3$ for 135 cutting angle.

3.2. Tool-material Interaction

Based on the analysis of the characteristic of the cutting forces, the chip formation is found to be changed as the increasing of RDD for both 90 and 135 cutting angles. Chip formation modes are dependent on the tool-material interaction in nature as shown in Figure 6.

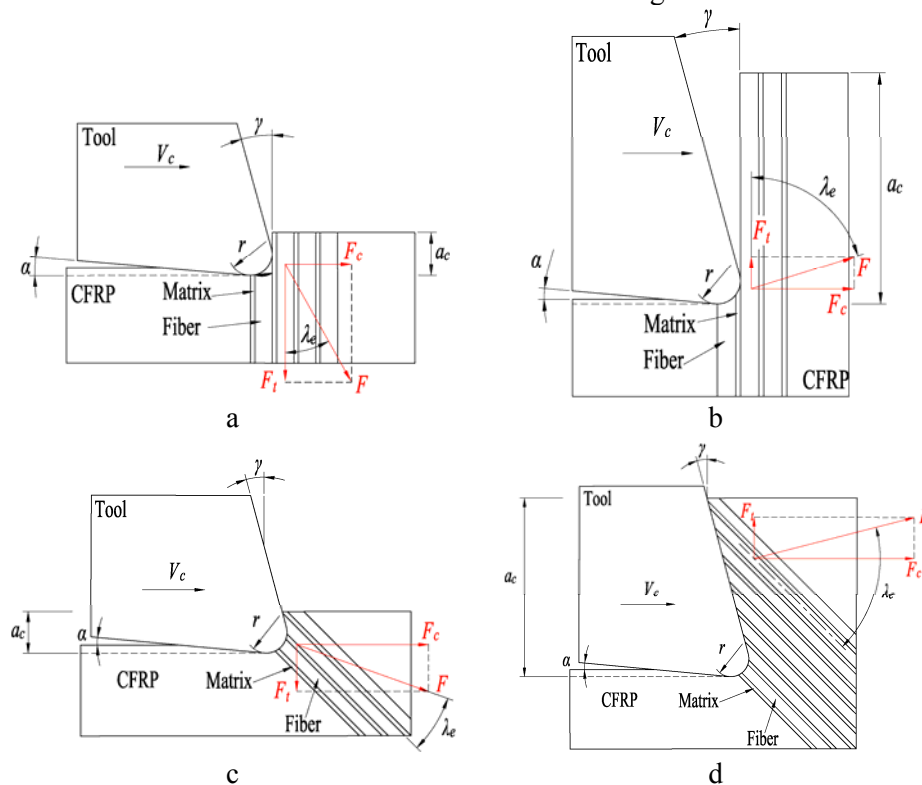


Figure 6. Tool-material interaction under different RDDs: a) RDD=1, $\theta=90^\circ$; b) RDD=5, $\theta=90^\circ$; c) RDD=1, $\theta=135^\circ$; d) RDD=5, $\theta=135^\circ$.

The angle formed by rotating from the resultant force to fiber orientation is defined as the angle of action (λ_e) to investigate the tool-material interaction. It has been noted that the chip formation mode for 90° cutting angle is cutting-dominant type in the literature. As shown in Figure 5 (a), the fact that the chip formation is the cutting-dominant type may be premised on the condition that the angle of action is larger than 45° for 90° cutting angle. Meanwhile, the angle of action becomes close to 90° with the increasing of RDD. It presents the resultant force is nearly perpendicular to the fiber as shown Figure 6(b). However, the angle of action is smaller than 45° when RDD=1. In this case, the resultant force direction is nearly along the fiber pointing in the work material as shown in Figure 6 (a). The fiber suffers the pressure of the cutting edge. As a results the chip formation mode changes into a buckling-dominant type instead of the cutting-dominant type accordingly.

In case of 135° cutting angle the chip formation consists of the compression after the large bending

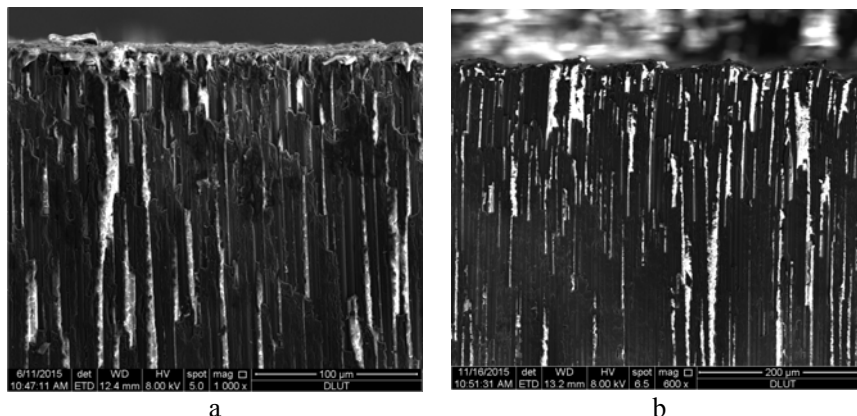
deformation of fibers. Unlike the case of 90° cutting angle, the fiber contacts the rake face firstly when $RDD \geq 3$. This is the same as the cantilever beam. It is more likely to cause mode I fracture with the increasing value of the component of the resultant force along the fiber. Figure 5(b) shows there are the same chip formation modes for both $RDD=3$ and $RDD=5$. However, the angle of action is smaller than 45° shows further evidence for that there is a press action of the cutting edge when $RDD=1$.

3.3. Failure mechanism in chip formation

Detailed examination of the machined surface is conducted by SEM to understand the failure mechanism of the fiber and the matrix in the process of chip formation. In case of $RDD=1$, there is no subsurface damage as shown in Figure 7(a, c). As discussed above, the specific thrust energy required for 90° cutting angle is far greater than the one for 135° cutting angle. Fibers are initially straight and well aligned for 90 cutting angle, have some resistance to bend due to the surrounding composite. Its failure point is above the cutting plane. The uncut fiber is pressed by the cutting edge. As a result, these fibers may crush in the manner of brittle material as shown in Figure 8(a). Its fracture morphology is the same as the one of the compression microbuckling under the unidirectional compressive load. However, the stiffness perpendicular to the fiber of the surrounding composite decreases for 135° cutting angle. Fibers may bend leading to a misalignment. In this case, the load by the cutting edge produce a shearing action on fibers. The energy required for this failure mode depends on the shearing strength of fibers. Thus, it needs less energy to failure than that for 90° cutting angle due to the large compressive strength of fibers.

As shown in Figure 7 (b), there is a V shape obviously in the machined surface. The direction of the long side of the V shape is nearly coincide with that of the resultant force. During machining, first a small crack develops at the tool tip due to the compression of the cutting edge. The crack extends along this direction forming a plane as shown very clearly in Figure 7(b), which consists of the kinkband of fibers. With the cutting edge cutting in the work material, the matrix is under the shear load due to the pushing of the rank face. It requires more energy to fracture than that under the opening load [18]. The chip separates from the work material until mode I fracture occurs at a plane in the interface along the fiber. Meanwhile, the long crack is obvious at the machined surface as shown in Figure 8(b), which distributed at equal distance corresponding to the subsurface damage as show in Figure 7(b). It is caused by mode I fracture of the interface due to the bending deformation of the fiber before the chip separation.

In case of 135° cutting angle fibers bend obviously with mode I fracture of the interface when $RDD \geq 3$ as shown in Figure 7(d). It is mainly caused by the pushing of the rank face as discussed in tool-material interaction. Furthermore, fibers easily bend without the restriction of the matrix due to mode I fracture. As shown in Figure 8(c) the fractographic features shown on the fiber ends exhibit the morphology of the tensile failure. Consequently, the bending deformation would trigger the tensile failure of fibers at the position where the radius of curvature of the fiber achieve the minimum. According to the theory of the cantilever beam the cantilever length becomes much longer with the increasing of the RDD. This process can induce the severe subsurface damage with the growth of hundreds times. Therefore, the fiber only be cut after the cutting edge contacts it as for 90° cutting angle.



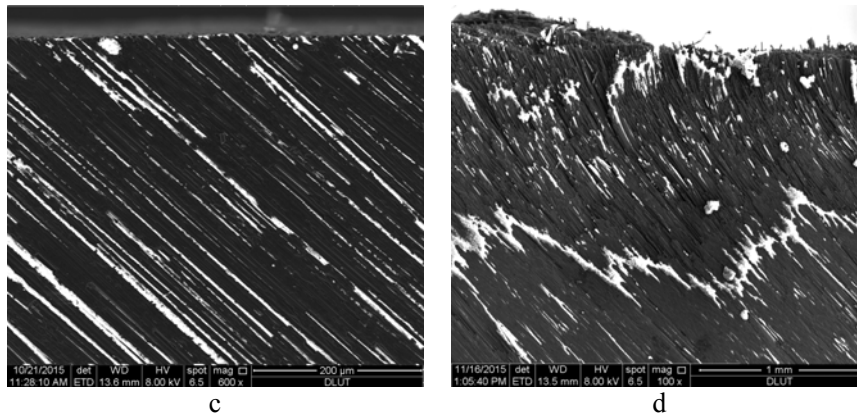


Figure 7. Subsurface damage under different RDDs: a) RDD=1, $\theta=90^\circ$; b) RDD=5, $\theta=90^\circ$; c) RDD=1, $\theta=135^\circ$; d) RDD=5, $\theta=135^\circ$.

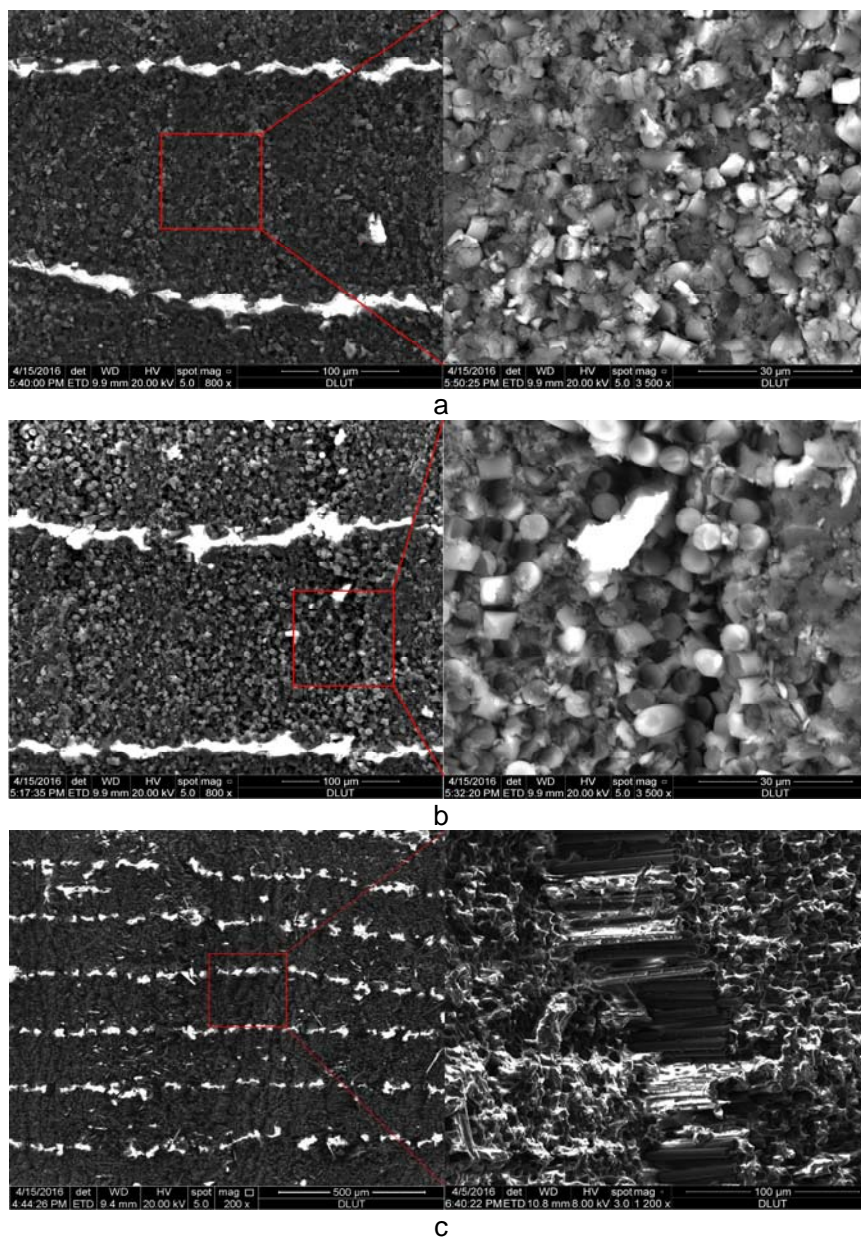


Figure 8. Failure micro topography of fibers under different RDDs: a) RDD=1, $\theta=90^\circ$; b) RDD=5, $\theta=90^\circ$

Excerpt from ISBN 978-3-00-053387-7

4. Conclusions

For 90° cutting angle, the chip formation of the cutting-dominant type is the repeated process consisting of the Mode I fracture of interface after a series of fiber kinking when $RDD \geq 3$. There is some subsurface damage due to the bending of fibers. However, in case of $RDD=1$ the chip formation is the process of the microbuckling due to the insufficient support of the matrix above the cutting plane, and the interface debonding does not extend to the subsurface. For 135° cutting angle, Mode I fracture of the interface easily occurs under the opening load with the large bending deformation when $RDD \geq 3$. Thus, the RDD should be controlled to reduce the severe subsurface damage in machining of CFRPs for 135° cutting angle especially.

Acknowledgments

The work is partly supported by the National Basic Research Program of China (grant number 2014CB046503), the Funds for Creative Research Groups of China (grant number 51321004); the National Natural Science Foundation of China (grant number 51505064, U1508207, 51575082).

References

- [1] D.F. Liu, Y.J. Tang, W.L. Cong. A review of mechanical drilling for composite laminates. *Composite Structure*, 94.4: 1265-1279, 2012.
- [2] C.R. Dandekar, Y.C. Shin. Modeling of machining of composite materials: a review. *International Journal of Machine tools and manufacture*, 57: 102-121, 2012.
- [3] Z.Y. Jia, Y.L. Su, B.Y. Zhang, C. Chen, F.J. Wang. The prediction of the cutting force in machining CFRP based on the RBF artificial neural network, *Acta Materiae Compositae Sinica*, 33.3: 516-524, 2016.(in Chinese).
- [4] D. Arola, and M. Ramulu. Net shape manufacturing and the performance of polymer composites under dynamic loads. *Experimental mechanics*, 37.4: 379-385, 1997.
- [5] P. Ghidossi, M.El. Mansori, F. Pierron, Influence of specimen preparation by machining on the failure of polymer matrix off-axis tensile coupons, *Composite Science Technology*, 66.11: 1857-1872, 2006.
- [6] H.Y. Pwu and H. Hocheng. Chip formation model of cutting fiber-reinforced plastics perpendicular to fiber axis. *Journal of manufacturing science and engineering*, 120.1: 192-196, 1998.
- [7] J.Y. Sheikh-Ahmad. Machining of polymer composites. Springer, New York, 2009.
- [8] A.S. Jahromi, B. Bahr, K.K. Krishnan. An analytical method for predicting damage zone in orthogonal machining of unidirectional composites. *Journal of Composite Materials*, 48.27: 3355-3365, 2014.
- [9] R. Rentsch. Crack formation and crack path in CFRP machining. *Proceedings of crack paths, Gaeta, Italy*, 2012.
- [10] CFRP Cutting Mechanism (3rd Report) Effects of Tool Edge Roundness and Relief Angle on Cutting Phenomena. *Journal of the Japan Society for Precision Engineering*, 57.3: 491-496, 1991.
- [11] X.M. Wang, L.C. Zhang. An experimental investigation into the orthogonal cutting of unidirectional fibre reinforced plastics. *International Journal of Machine tools and manufacture*, 43.10: 1015-1022, 2003.
- [12] A.S. Jahromi, B. Bahr. An analytical method for predicting cutting forces in orthogonal machining of unidirectional composites. *Composites Science and Technology*, 70.16: 2290-2297, 2010.
- [13] Q. An, W. Ming, X. Cai, M. Chen. Effects of tool parameters on cutting force in orthogonal machining of T700/LT03A unidirectional carbon fiber reinforced polymer laminates. *Journal of Reinforced Plastics and Composites*, 34.7: 591-602, 2015.
- [14] R. Teti, Machining of composite materials, *CIRP Ann-Manuf Techn*, 51.2 (2002): 611-634.
- [15] Greenhalgh, Emile. Failure analysis and fractography of polymer composites. Elsevier, London, 2009.